International Journal of Information, Control and Computer Sciences
ISSN: 2517-9942
Vol:11, No:4, 2017

Enhanced Multi-Intensity Analysis in Multi-Scenery Classification-Based Macro and Micro Elements

R. Bremananth

Abstract—Several computationally challenging issues are encountered while classifying complex natural scenes. In this paper, we address the problems that are encountered in rotation invariance with multi-intensity analysis for multi-scene overlapping. In the present literature, various algorithms proposed techniques for multi-intensity analysis, but there are several restrictions in these algorithms while deploying them in multi-scene overlapping classifications. In order to resolve the problem of multi-scenery overlapping classifications, we present a framework that is based on macro and micro basis functions. This algorithm conquers the minimum classification false alarm while pigeonholing multi-scene overlapping. Furthermore, a quadrangle multi-intensity decay is invoked. Several parameters are utilized to analyze invariance for multi-scenery classifications such as rotation, classification, correlation, contrast, homogeneity, and energy. Benchmark datasets were collected for complex natural scenes and experimented for the framework. The results depict that the framework achieves a significant improvement on gray-level matrix of co-occurrence features for overlapping in diverse degree of orientations while pigeonholing multi-scene overlapping.

Keywords—Automatic classification, contrast, homogeneity, invariant analysis, multi-scene analysis, overlapping

I. Introduction

MULTI-INTENSITY analysis (MIA) in multi-scenery classification and pattern analysis is an important task performed to address problems when diverse anisotropic or isotropic patterns occur in textures. Most of the applications of MIA in computer vision, image processing, multimedia, and medical image analysis [1], [19], [20] are required to enhance the framework of multi-scenery classification. However, the physical properties and frequency components of anisotropic textures are frequently modified. On the other hand, frequency components of isotropic textures are not altered substantially at diverse orientations. Isotropic textures provide the same physical properties in all directions [12], [20]. Algorithms that are currently available are extended to other varieties of applications such as medical image analysis, industrial automation, biomedical image processing, remote sensing, and other related fields [1]-[4]. In the field of invariant pattern analysis (IPA), MIA plays a vital role in making a classification of inter- and intra-patterns obtained from the complex scene with diverse signals in diverse angle variations.

In general, natural and non-natural patterns are obtained from any two-dimensional scene with different signal variations [15]. They fit in either anisotropic or isotropic classifications based on their interior formations. The anisotropic textures have physical characteristics that are different in diverse directions, and their frequency components modify significantly in dissimilar directions. However, isotropic textures provide the same physical properties in all directions, and their frequency components do not alter appreciably at diverse orientations. MIA provides a significant requirement for pattern analysis and distinguishes the overlapped objects. Furthermore, in texture features analysis, MIA utilizes to achieve high inter-class discrimination while less intra-class unpredictability stumbles upon the patterns [15].

Several works were proposed using MIA for IPA in the current literature [1], [2], [8], [19]. However, the problem of MIA-based location [5], rotation, and scale IPA is still an open issue for various real-world computer vision applications. The ultimate aim of all the previously proposed algorithms is to enhance the classification efficacy instead of fulfilling transformation invariants. This is our motivation in this paper– to present a framework for MIA. In addition, work here is also an enhanced version of our previous paper [1], [19].

Generally, texture analysis is categorized into two types: Structural [5] and statistical [6], [7] texture analysis. In the structural approach, the active-region-of-interest (AROI) is taken as a pool of picture elements and its property texture is utilized in order to classify similar active objects [8], [9], [18]. However, IPA can be performed by the sequence-of-chain of connections in the AROI for each frame appearing in a multi-scenery classification. A chain of connections is an essential feature to obtain better classification efficacy. Based on diverse poses of each frame appearing in a scene, the computing parameters are: asymmetrical, arbitrariness, clumsiness, gaucherie, hardness, inelegance, sheerness, and stiffness [1], [10], [19]. In the statistical texture analysis, the properties of texture AROI are compared with the pixel of reference regions. Normally, statistical algorithms have Fourier transforms, wavelets, convolution filters, co-occurrence matrix, spatial autocorrelation, and fractals [13], [14]. A fusion approach of both methods is required where larger diverse characteristics appear in the texture.

In this paper, we present a framework for MIA that is based on [1], [19]. This algorithm belongs to the category of a fusion approach that includes the characteristics of detecting macro and micro texture elements (TE). Once the boundaries of the TE are identified, a block of TEs is grouped together based on its structural, primeval, and spatial measures. The primeval size and its spatial interconnection of TE are concerned with a confined environ of pixels [1]. A set of ill-connected TEs is called Micro-Texture-Elements (MITE). On the other hand, if a set of TEs has a divergent silhouette and habitual association of connections, then those TEs are referred to as

Bremananth Ramachandran is with the Information Systems and Technology Department, Sur University College, Sur, P. O.Box 440, PC. 411, Sultanate of Oman (e-mail: bremananth@suc.edu.om).

Macro-Texture-Elements (MATE).

MITE and MATE are the vital parameters for enhanced multi-intensity analysis (EMIA) [1], [11], [19]. The properties of anisotropic or isotropic textures' intensity are associated with MITEs and MATEs when the intensity varies from micro to macro. A group of TEs is analyzed for the classification of texture patterns. Based on fundamental characteristics that appear in the structural, primeval, and spatial measures in the TE, the structure and statistical multi-intensity analysis method works to enhance the feature extraction of textures and address the problem of minimizing the overlap of visibility and maximizing the classification accuracy.

The remainder of this paper has been organized as follows: Section II describes the framework for EMIA. Section III illustrates the results and analysis of the framework, and the concluding remarks are presented in Section IV.

II. Framework for EMIA

Fig. 1 shows the framework of EMIA. This framework has three phases. In first phase, a sequence of operations is performed including MIA ratio analysis, computation of minimum area window of overlap, and calculation of cumulative deviation textures. A basis function has been formulated based on the result obtained in the first phase. The basis function, boundary of TE construction, and intensity deviation with minimum AROI are the sequence of operations performed in the second phase of the framework. The third phase computes quadrangle Block-of-Pixel (BOP), MITE and MATE statistical analysis, and MIA aliasing.

A. Ratio Analysis

Assume that N sets of Block-of-Windows (BOW) appear in the texture portion. The middle portion of the BOW consists of a set of coordinates that are represented as (Φ_j, Ψ_j) , $j = 1, \cdots N$. The principal BOWs are denoted as (Φ_j^p, Ψ_j^p), $j = 1, \cdots N$. In a BOW, the upper-left and lower-right coordinates are represented as (Ψ_m, Ψ_n) and (Φ_m, Φ_n), respectively. For simplicity, the BOW size can be represented by its radius Υ_j $j = 1, \cdots N$ and two corners of the BOW size are characterized as Υ_m, Υ_n. The MIA ratio has been analyzed based on aforesaid properties.

B. Block-of-Windows Overlapping

Computing the minimum area BOW overlap is mainly for obtaining the basis function of this framework. Three factors are primarily involved in the basis function formulation such as MIA ratio of the texture, a minimum area of BOW, and cumulative deviation from the primarily position of BOW. The minimum area BOW has been computed by finding the ratio between two primary BOW coordinate positions (Ψ_m, Ψ_n) and (Φ_m, Φ_n). In order to compute minimum overlap positions, a process of merely moving the BOW is required in the middle portion of the texture.

C. Textures Deviation

In anisotropic or isotropic texture patterns, a larger divergence appears because its primary coordinates deviate significantly. In the computation of cumulative deviation, it is an essential process to consider the MIA minimum and maximum ratios and area of the BOW overlap. Obviously, BOW size cannot be capricious due to the nature of its texture in MIA. Consequently, the primary deviation of appearance of the BOW is assumed to be Υ_j^p and its sequence is Υ_m, $j = 1, \cdots N$.

D. Basis Function Formulation

Formulation of a basis function is based on three factors: MIA ratio of the texture, a minimum area of BOW, and cumulative deviation from the primarily position of BOW. The basis function has been designed as a linear arrangement of the individual basis function that is based on the parameter [1],

$$\Gamma \quad = \quad \ell(b) + \delta\psi\eta(b) + \upsilon(b),\ b = 1 \cdots m, \tag{1}$$

where m denotes the number of BOW, $\ell(b), \eta(b)$ and $\upsilon(b)$ represent the MIA ratio, minimum area the BOW overlap, and cumulative deviation, respectively, while ψ is a scaling factor used to compute the minimum area of the BOW overlap. The parameter δ represents weight for the diverse overlapping of BOW, and Γ denotes MIA intensity on overlapping of BOW in AROI.

The basis function of EMIA is defined as

$$\ell(b) \quad = \quad \sum_{g=1}^{N} \eta_g(b),\ b = 1 \cdots m, \tag{2}$$

$$\eta(b) \quad = \quad \begin{cases} 1 - e^{-\tau^2/\sigma}, & \text{if } |\tau| > 0, \\ 1/2, & \text{if } |\tau| = 0, \\ 0, & \text{if } |\tau| < 0, \end{cases} \tag{3}$$

where τ is an appraisal of BOW overlapping and σ denotes a bend factor for controlling EMIA.

$$\upsilon(b) \quad = \quad \sum_{i=1}^{N} \varrho_i(b),\ b = 1 \cdots m. \tag{4}$$

E. Construction of Texture Elements

Locality and topology are important parameters when MIA is performed on the texture features. These two parameters are primarily involved in the property of TE when BOP consistently appears in the BOW. Generally, BOP is a set of TE that constitutes a meaningful property when texture features are encountered.

TE property constitutes based on two main factors such as the shape of its BOP and basis function formulation. The boundary of the TE is mainly based on BOW texture overlap. The overlap of textures normally has a combination of hidden areas. Recovering these hidden texture patterns from the overlapped portion is a challenging task. It can be done

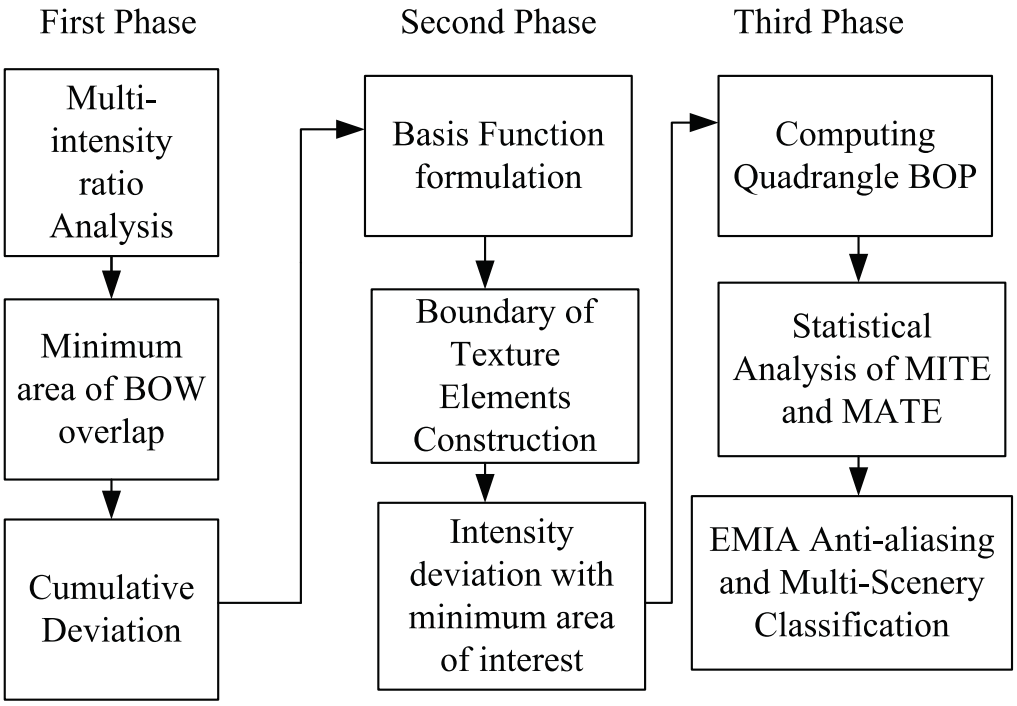

Fig. 1 A proposed framework for enhanced multi-intensity analysis

by sampling its signals into a sequence of quadrangles. The sampling error is also compensable. That is why, we have chosen the TEs for EMIA in the connected neighboring of pixels. The EMIA of textures is viewed as a tessellation of the quadrangle. The diverse area is a loosely or logically connected BOW. A tessellation is a method for generating a 2D plane. It reoccurs in the geometric quadrangle or other shapes with roughly no overlaps and fissures [1], [19].

Any overlapped TE textures can be decayed into a set of intensity approximation pixels. Each BOW consists of quadrangle TEs of the same size. In the diverse overlapped BOW, every TE may have different connected components of BOP. They are contributed diverse natures of features.

In the boundary TE construction, we have to consider the overlapped diverse textures. The quantity of its patterns may have analogous properties or related characteristics. However, the TE can have a huge divergence of nature and provide the entire difference in the overlapping locations [1]. EMIA for the TE construction analysis is required to improve the discrepancies in texture intensities.

From (1), Γ provides EMIA deviation on the overlapping of AROI. It has $\ell(b)$, $\delta\psi\eta(b)$, and $\upsilon(b)$. The minimum area BOW overlap is controlled by δ. The boundary TE construction is based on the overlapping of intensity on the texture. Based on research, we found that δ has to be assumed, as in (5), when boundary TE construction is carried out. The computation result of first phase in the framework and basis function is involved in the construction of the TE boundary.

$$\rho = \begin{cases} 0.1, & \text{if } \delta = 0, \\ 0.5, & \text{if } \delta > 0, \\ 0.9, & \text{if } \delta < 0. \end{cases} \quad (5)$$

F. Minimum AROI Intensity Deviation

The minimum AROI for intensity deviation is another important task in the framework. Once the texture pattern is materialized on AROI. It is decayed into a set of intensities of diverse BOW, and each BOW consists of a BOP quadrangle. Intensity contribution of each quadrangles has a diverse TE. For this reason, intensity deviation with minimum AROI requires a connected TE arrangement for each BOP. Perhaps, two dissimilar TEs with diverse intensities may be exactly similar or entirely diverse. Moreover, the scattering of intensity deviation in the texture patterns, especially on the overlapping BOW, is required for the analysis of TE and its variance. The intensity deviation λ denotes the following in (6).

$$\lambda = \begin{cases} m_b(i,j) = 0, & \text{if } i > m || j > n, \\ m_b(i,j) = i_{mg}(i,j)\delta, & \text{if } otherwise. \end{cases} \quad (6)$$

G. Quadrangle BOP

Quadrangle BOP is computed based on the spatial TE relative to the plane surface of the texture. We can identify

the BOP whether it appears inside or outside or not on the TE BOP at all. It is described in (7).

$$\chi = \begin{cases} not\ on, & \text{if } Ax+By+Cz+d <> 0, \\ inside, & \text{if } Ax+By+Cz+d < 0, \\ outside, & \text{if } Ax+By+Cz+d < 0, \end{cases} \quad (7)$$

The hierarchy of quadrangle BOPs is utilized to represent three dimensional space. Medical imaging and other automation computer vision applications that require Quadrangle BOP cross sections [17].

H. MITE and MATE Statistical Analysis

Statistical analysis of MITE and MATE is a computationally challenging task for building MIA pixel regions. The statistical relationship between MITE and MATE for BOW can be computed based on the quadrangle of BOP and its neighboring signals. The mean of MITE and MATE is computed and described as

$$\mu = \frac{\sum_{i=1}^{\lambda}\sum_{j=1}^{\lambda} m_b(i,j)}{\kappa^2}. \quad (8)$$

The variance computation of MITE and MATE is described as

$$\nu = \frac{\sum_{i=1}^{\lambda}\sum_{j=1}^{\lambda}[abs(m_b(i,j)) - \mu]}{\lambda^2}. \quad (9)$$

The standard deviation computation of MITE and MATE is described as

$$\sigma = \sqrt{\nu}. \quad (10)$$

I. Aliasing on EMIA

In EMIA, when texture patterns are sampled, an aliasing effect causes diverse signals to be indistinguishable. This distortion appears when certain consequences occur in the reconstructed signals. BOW and BOP signals are different from the discrete samples and the original continuous signals in BOP variations [13].

The computation of anti-aliasing makes the EMIA texture signals more distinguishable when compared to the normal analysis. As per the Nyquist sampling rate, the minimum sampling rate is required to avoid the aliasing effect, especially in texture signals. The sampling rate is normally double the highest frequency (h_f), which is encountered in non-zero intensities, i.e., $N_r = 2h_f$.

In general, sampling can be either in the temporal or spatial domain. EMIA anti-aliasing is mainly concerned with the spatial domain. Therefore, the space domain of texture patterns are considered. In the time domain, sampling is in time Δt and the Nyquist frequency is computed as $N_f = 1/2\Delta t$, whereas in the spacial domain, the BOP distance is Δ and Nyquist wavenumber becomes $N_k = \frac{1}{2}\frac{2\pi}{\Delta} = \frac{\pi}{\Delta}$.

If the measured BOP frequency is higher than the Nyquist frequency, then it will be folded back to the lower frequency. In order to properly make spatial signals among the BOP more distinguishable, we have to avoid the spatial aliasing among the intensity variations, which means that the constraint $N_k > k$ should be satisfied. Thus, the minimum BOP space is represented as $\Delta = \lambda/2$, where λ represents the wavelength of the signal.

In EMIA, artifacts appear in the textures when signal variations occur on the discrete sampling. It was also affected by the errors due to discrete measurements. In order to avoid aliasing between the BOP, we require the Nyquist constraint. Furthermore, texture BOP separation Δ should also be less than the distance between the measurement and source m_d, aperture as $\Delta < m_d$. Based on research, if a spatial wave length (λ) is 0.2, then BOP spacing becomes $\Delta = 0.2/2 = 0.1$ m. A hologram is required for PSNR. If it could be 60dB and the spatial resolution is 0.1 m, then the spatial distance is computed as $m_d < (0.1 * 60)/27.2875271(20 * pi * log(e)) = 0.21098 \approx 0.2$ and BOP spacing should have a constraint of 0.1 m < 0.2 m.

III. EMIA Implementation and Result Analysis

Benchmark data sets have been collected to test the algorithms of the proposed framework. Algorithms are implemented, debugged, and tested in MATLAB with diverse textures. Experiments have been carried out in three phases of the framework. EMIA of overlap textures was analyzed with different odd numbers of intensity factors $\lambda = 1, 3, 5, ..., 15$. The results reveal that multi-intensity of textures is confined when λ is incremented by an odd number of factors. While applying an even number of intensity factors, they also provide the same effect in the texture patterns.

In multi-scenery classification, gray-level matrix of co-occurrence features (GMCF) can be employed to classify the distinct patterns [16]. Furthermore, results disclose that these feature sets can improve the performance of EMIA. Based on the performance metrics such as contrast, homogeneity, correlation, and energy, 20–30% of more performance was given by EMIA than the MIA [1][19]. Fig. 2 shows multi-scenery EMIA textures with intensity factors λ from 1 to 15, by step 2.

A. Contrast Metrics

An intensity contrast C_m metric is employed to measure the performance between BOW and its neighbors over the entire dimension of the textures. The contrast metric C_m is described as

$$C_m = \sum_{i=1}^{n}\sum_{j=1}^{n} |BOW_i - BOW_j|^2 G_{bow}(i,j). \quad (11)$$

Contrast metric of texture feature was measured based on tests performed with 220 data sets. The mean of minimum contrast was 1.1012, and the maximum mean contrast was 0.71121. In Table I, the first row exemplifies contrast metrics. It reveals that the EMIA framework significantly reduced textures' contrast and made them suitable for multi-scenery classifications.

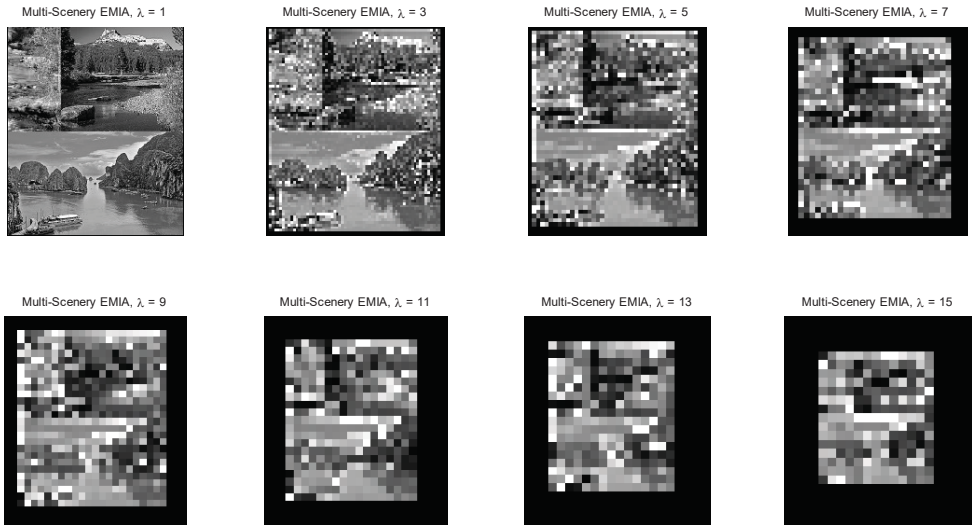

Fig. 2 Multi-scenery EMIA textures with intensity factors λ from 1 to 15, by step 2

TABLE I
MIA [1] AND EMIA [19] MEASURES OF METRICS

Properties	Min. MIA[1]	Max. MIA[1]	Min. EMIA[19]	Max. EMIA[19]
Contrast	1.2099	0.7491	1.1012	0.71121
Homogeneity	0.9459	0.9636	0.9632	0.9833
Correlation	0.9334	0.9587	0.9532	0.9872
Energy	0.3322	0.3427	0.6434	0.7387

B. Homogeneity Metrics for EMIA

Homogeneity is a metric. It is employed to measure the intensity proximity of the distribution of BOP. The quadrangle of the GMCF can be measured by homogeneity metrics. These features also represent texture diagonals and the unique signal variations of the textures as well. This is described as

$$H_m = \sum_{i=1}^{n}\sum_{j=1}^{n}\frac{G_{bow}(i,j)}{1+|BOW_i - BOW_j|}. \quad (12)$$

The minimum and maximum homogeneity H_m of texture features were 0.9632 and 0.9833, respectively. Homogeneity for EMIA reveals that the minimum and maximum distribution of BOP were improved significantly when compared to that of MIA. This is depicted in the second row of Table I.

C. EMIA Correlation Metrics

Correlation metric is a measure of the MIA that has been analyzed as

$$R_m = \sum_{i=1}^{n}\sum_{j=1}^{n}\frac{(BOW_i - \mu_i)(BOW_i - \mu_j)G_{bow}(i,j)}{\sigma_{BOW_i}\sigma_{BOW_j}}. \quad (13)$$

The minimum and maximum EMIA's correlation R_m was 0.9532 and 0.9872, respectively. The results reveal that minimum and maximum GMCF correlation have been improved significantly. The third row of Table I is depicted for correlation metrics.

D. EMIA Energy Metrics

The sum of the square of GMCF is called energy of the EMIA. This is described as

$$e_m = \sum_{i=1}^{n}\sum_{j=1}^{n} G_{bow}(i,j)^2. \quad (14)$$

The minimum and maximum MIAs of energy e_m were 0.6434 and 0.7387, respectively. These measures reveal that minimum and maximum GMCF energies were improved significantly. In Table I, the fourth row depicts the energy metrics.

E. Diverse Intensity Factors Analysis

In the result analysis, multi-scenery textures were analyzed with EMIA algorithms. Intensity factors (λ) have been incremented from 1 to 15 by step 2 for the analysis of diverse texture behaviors. BOW of GMCF was rotated in diverse angles for analysis. The results are shown in Fig. 3 with $\theta = 135^o$. They reveal that if λ is increased, then its texture measures such as correlation, energy, homogeneity metrics are also improved significantly. Furthermore, texture contrast was minimized considerably. Fig. 6 depicts comparative result of the previous approach MIA [1][19] and proposed EMIA framework of this paper. Four metrics were analyzed based on the result of the EMIA framework. The minimum and maximum intensity variations were observed. The results disclose that the performance of the proposed method has enhanced multi-scenery texture features.

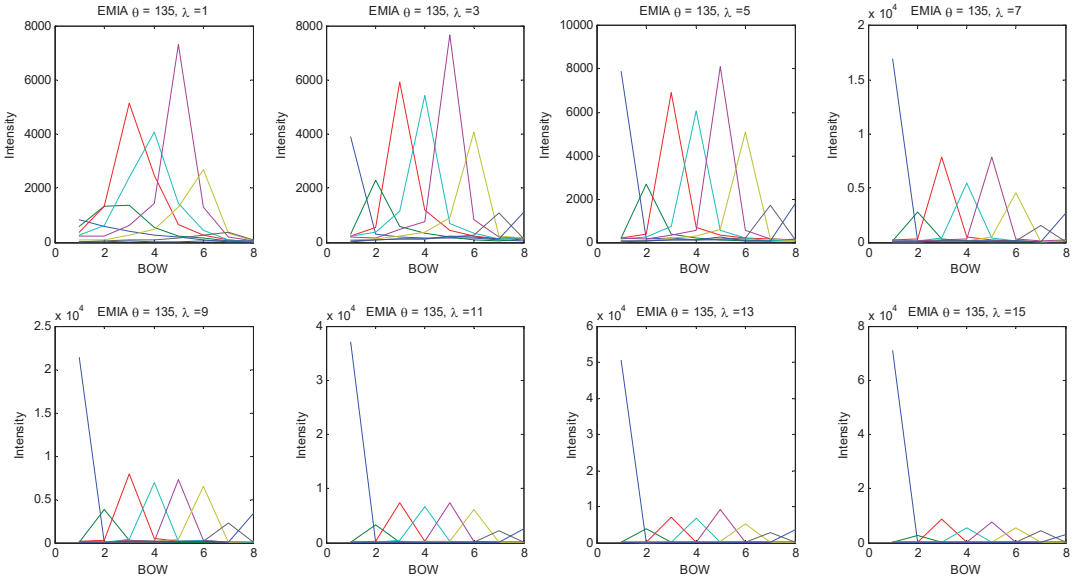

Fig. 3 Result of multi-scenery EMIA textures with odd number of intensity factors λ from 1 to 15, by step 2 and $\theta = 135$.

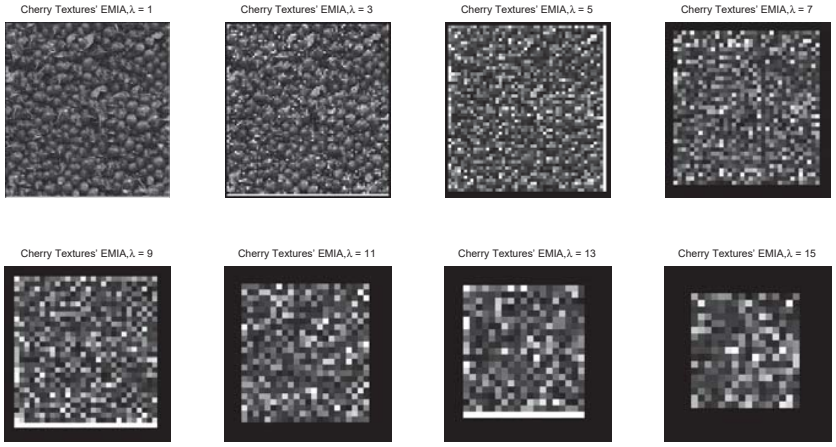

Fig. 4 EMIA of three overlapping textures with different even number of intensity factors

IV. Conclusion

The problem of the multi-scenery taxonomy in diverse rotation has been addressed in this paper by applying a framework of enhanced multi-intensity analysis. This framework consists of micro and micro basis functions. These functions have aptly enhanced and been applied in natural multi-scene classifications and its overlapping pattern. We found that this framework conquered the minimum classification false alarm while pigeonholing the problematic overlapped multi-scene patterns. In addition, a quadrangle multi-intensity decay was invoked to resolve the MIA inconsistences. To reveal the efficacy, rotation-invariant, classification, correlation, contrast, homogeneity, and energy parameters were utilized to analyze invariants. The computed BOP was utilized to locate the overlapping regions in order to minimize classification and maximize the rendered visibility. Based on BOP, for minimizing multi-BOW, the textures were decayed into a quadrangle. The parameters such as rotation, classification, correlation, contrast, homogeneity, and energy were utilized to analyze invariant for multi-scenery classifications. Metrics' results reveal that the proposed framework is suitable to be incorporated in a multi-BOW environment and other multi-scenery classifications. In the near future, a view of n-dimensional BOW perception-based online training of BOW will be suggested to estimate the

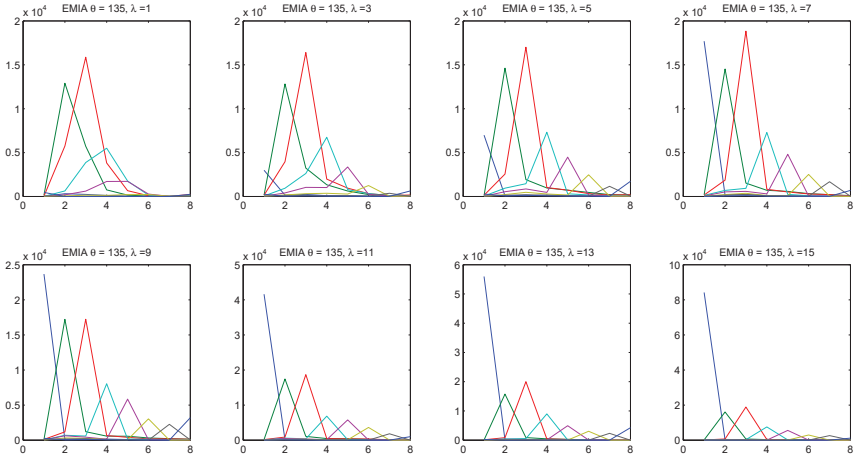

Fig. 5 EMIA of overlapping textures for GMCF from 1 to 8 for three overlapping textures

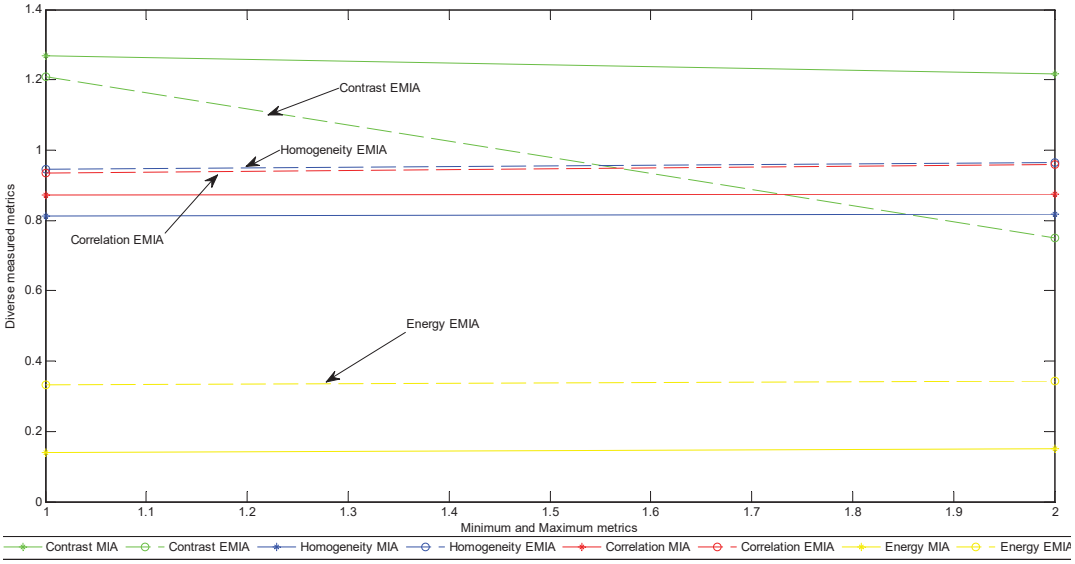

Fig. 6 MIA [1] and EMIA [19] metrics comparison

diverse intensity variations of textures.

Acknowledgment

The author would like to thank the management of Sur University College for providing the necessary support while carrying out this research in a successful manner.

References

[1] R. Bremananth, "Multi-intensity analysis for overlapping of invariant textures in mobile communications," *Inte. Conf. on Advances in Mobile Network, Communication and its Applications*, 2012. © IEEE: 978-0-7695-4720-6/12. doi:10.1109/MNCApps.2012.10.

[2] D. Wal et al., "Characterisation of surface roughnessand sediment texture of intertidal flats using ERS SAR imagery," *Remote Sens. Environ.*, vol. 98, no. 1, pp. 96–109, Sep. 2005.

[3] T. Menpa et al., "Real-time surface inspection by texture," *Real Time Imaging*, vol. 9, no. 5, pp. 289–296, Oct. 2003.

[4] W. M. Chen et al., "3-D ultrasound texture classification using run difference matrix," *Ultrasound in Med. & Biol.*, vol. 31, no. 6, pp. 763–770, Jun. 2005.

[5] B. Verma and S. Kulkarni, "A fuzzy-neural approach for interpretation and fusion of colour and texture features for CBIR systems," *Appl. Soft Comput.*, vol. 5, no. 1, pp. 119–130, Dec. 2004.

[6] T. Ojala et al., "Multiresolution gray-scale and rotation invariant texture classification with local binary patterns," *IEEE Trans. Pattern Anal. Machine Intell.*, vol. 24, no. 7, pp.971–987, Jul. 2002.

[7] J. L. Chen, "Rotation and gray scale transform invariant texture identification using wavelet decomposition and hidden markov model", *IEEE Trans. Pattern Anal. Machine Intell.*, vol. 16, no. 2, pp. 208–214,

Feb. 1994.
[8] Q. Song, "A new multi-scale texture analysis with structural texel,", CSIE 2011, Part I, CCIS 152, pp. 61–66, 2011.
[9] J. R. Smith and S. F. Chang, "Automated binary texture feature image retrieval," *Proc. IEEE Intl. Conf. Acoust., Speech, and Signal Proc.*, Atlanta, GA, 1996. © IEEE:1520-6149. doi:10.1109.
[10] J. R. Smith and S. F. Chang, "Transform features for texture classification and discrimination on large image database," *Proc. IEEE Intl. Conf. on Image Proc.*, 1994. © IEEE:1520-6149. doi:10.1109/ICIP.1994.413817.
[11] Q. Tian et al., "Display optimization for image browsing,", MDIC 2001, LNCS 2184, pp. 167–176, 2001.
[12] X. S. Zhou et al., "Water-filling algorithm: A novel way for image feature extraction based on edge maps," *Proc. IEEE Intl. Conf. On Image Proc.*, Japan, 1999. © IEEE. doi:10.1109/ICIP.1999.822959.
[13] G. N. Srinivasan, and G. Shobha, "Statistical texture analysis," *Proc. of World Academy of Science, Engg. and Tech.*, vol.36, pp. 1264–1269, Dec. 2008.
[14] R. Bremananth et al., "Wood species recognition system," *Int. J. of Comp., Elec., Auto., Cont. and Inf. Eng.*, vol. 3, no. 4, pp. 1138-1144, 2009.
[15] R. Bremananth et al., "On-line rotation invariant estimation and recognition," *Inte. J. on Advanced Computer Science and Applications*, vol. 1, no.2, pp.41–50, 2010.
[16] R. Bremananth et al., "Wood species recognition using GLCM and correlation," *Proc.of IEEE Computer society, Int. Conf. on Advances in Recent Technologies in Communication and Computing*, 2009, pp. 615–619. © IEEE: 978-0-7695-3845-7/09. doi:10.1109/ARTCom.2009.10.
[17] D. Hearn and M. P. Baker, *Computer Graphics C Version*, 2nd ed. Book, Prentice Hall, 1997.
[18] R. Bremananth et al., "An efficient superposition of acoustic field reconstruction in NAH," *6th Int. Conf. on Information and Communication Systems*, 2015, pp. 245250. © IEEE. doi:10.1109/IACS.2015.7103183.
[19] R. Bremananth and H. K. H. Abujalban, "A robust framework for enhanced multi-intensity analysis in multi-scenery classification," *IEEE Jordan Conference on Applied Electrical Engineering and Computing Technologies*, Jordan 2015, © IEEE: 2015 978-1-4799-7431-3/15/.
[20] R. Bremanath, "A study on transformation invariant pattern recognition," Ph.D. dissertation, Comp. Sci. Engg. Dept., Anna Univ., Chennai, Madras, 2006.

Bremananth R received his Bachelor's and Master's in Computer Science from Madurai Kamaraj and Bharathidsan University in 1991 and 1993, respectively. He obtained a Master of Philosophy degree in Computer Science and Engineering from Government College of Technology, Bharathiar University, in 2002. He received his Doctor of Philosophy degree in 2008 from the Department of Computer Science and Engineering, PSG College of Technology, Anna University, Chennai, India. He has completed his Post-doctoral Research Fellowship (PDF) from the School of Electrical and Electronic Engineering, Information Engineering (Div.) at Nanyang Technological University (NTU), Singapore, 2011. Before joining NTU, Singapore, he was a professor and head of the department of Computer Science and Application, in India. He has more than 23 years of experience in teaching, research, and software development at various institutions. Currently, he is an Associate Professor of Information Technology at the Information Systems and Technology Department, Sur University College, Sur, Oman, which is affiliated to Bond University, Australia. He is an associate editor of various international journals in the USA and an active reviewer of various IEEE international conferences/journals. His fields of research are acoustic holography, acoustic imaging, pattern recognition, computer vision, image processing, biometrics, multimedia, computer network, software engineering, soft computing, and microprocessors.

Dr. Bremananth received the M N Saha Memorial Award for the Best Application Oriented Paper in the year 2006 from the Institute of Electronics and Telecommunication Engineers (IETE). His continuous contribution to research was recognized by *Who's Who in the World*, USA, and his biography was published in the year 2006. He is a member of the Indian Society of Technical Education (ISTE), Advanced Computing Society (ACS), International Association of Computer Science and Information Technology (IACIT), and Institute of Electronics and Telecommunication Engineers (IETE).